Towards Using Radiation Damping to Improve Sensitivity

David Rourke, Seth Bush, Erwin Hahn, and Matthew Augustine
University of California, Davis, CA 95616

Field Inhomogeneity

Transcendental Solution

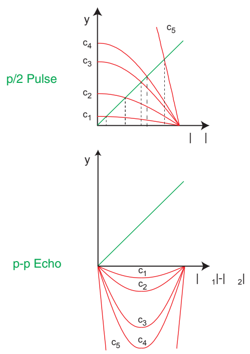

Radiation damping dynamics in both narrow line and homogenously broadened systems are well undestood. Introduction of magnetic field inhomogeneity necessarily complicates the radiation damping problem, and consequently, a complete analytical description has not yet been demonstrated. Initial work in this area led to a relationship between the initial tipping angle q_0 of the on resonance central vector of a symmetric field distribution M(0,t) and the change in tipping angle |Dq| due to the combined torque of radiation damping and the inhomogeneous magnetic field. The resulting area theorem generated from the Bloch equations using a transformation first realized in the treatment of self-induced transparency in optical systems can be written in terms of the radiation damping rate $1/T_R = 2pM_0Qgx$ and the inverse linewidth for a Lorentzian distribution T_2^* as

$$|Dq| = (T_2^*/T_R)\sin(q_0 - |Dq|).$$

This angle change |Dq| also represents the area of the measured time domain signall following a q_0 rf pulse. Graphical solutions to this transcendental equation for $q_0 = p/2$ and several choices of $c_n = T_2^*/T_R$ are shown on the top left. The diagram shown on the top right describes the net effect of the rotation of M(0,t) from the v direction at t = 0 to the M_z direction at a time later when all of the effects of radiation damping have vanished. Extension of this analytical approach to two and many rf pulses yields a series of transcendental relations such as that shown above. In the special case of two p rf pulses separated by a time long enough for radiation damping to vanish, one recovers the relation

$$|Dq_2| - |Dq_1| = -(T_2^*/T_R)\sin(|Dq_2| - |Dq_1|).$$

Graphical solutions to this equation are shown on the lower left for various choices of c_n. Since intersection of the linear curve representing $y = |Dq_2| - |Dq_1|$ with any of the curves $y = -(T_2^*/T_R)\sin(|Dq_2| - |Dq_1|)$ only ocurrs at the origin, $|Dq_2| = |Dq_1|$. The consequences of this equality are shown beginning with the middle diagram on the right. Following a p rf pulse M(0,t) at t = 0 is aligned along the $-M_z$ direction as shown by the green arrow. The combined effect of radiation damping and field inhomogeneity rotate M(0,t=0) toward the $+M_z$ diretion by an angle $|Dq_1|$ as shown by the red arrow. Application of a second p rf pulse transforms the red arrow into the green arrow shown in the diagram on the lower right. Again radiation damping and the inhomogeneous field rotate this vector to the +Mz direction due to the equality $|Dq_2| = |Dq_1|$. Although only appropriate for M(0,t), this theorem serves as a guide to the development of a three component echo. Indeed both

Vector Model

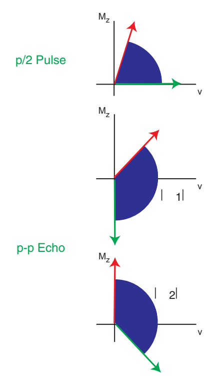

SEDOR Analogue

Sphere Hopping

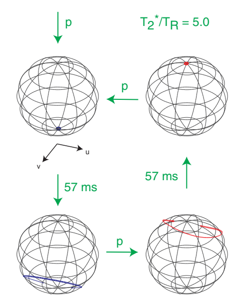

Although the analytical theorem is only appropriate for describing total rotation angles $|Dq_0|$ for M(0,t) from t = 0 until times when the reaction field due to all of the isochromats is averaged to zero, the idea of three component refocusing predicted by this theorem can be used as an indirect detector. The diagram on the left is appropriate for a symmetric Lorentzian distribution having $T_2^*/T_R = 5.0$. An initial p rf pulse inverts all of the isochromatic vectors, designated by a blue spot at the south pole of the sphere shown on the top left. After 57 ms, the vectors have fanned out in three dimensions shown on the bottom left sphere. For this particular choice of T_2^*/T_R, 57 ms corresponds to the maximum integrated transverse magnetization or signal. Application of a second p pulse transforms this distribution into the sphere shown on the bottom right. As time proceeds

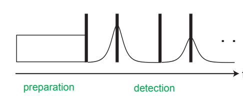

Continued application of this double p pulse train will cycle through these four spheres and the corresponding signal will decay according to a rate that is a function of T_1 and T_2. Clearly any departure from a symmetric distribution will alter the complete refocusing of the magnetization along $+M_z$ and be manifest in a change of the echo envelope. An example of such a sequence is shown above. Here one examines the decay of the double p echo train with and without any preparation pulses. The preparation pulses could be any double resonance experiment that perturbs the ^1H spectrum of a solute while leaving the solvent unaffected. To test this idea a sample of H_2O was chosen and the preparation period consisted of a hole burning experiment. The results shown on the right are appropriate for a symmetric Lorentzian distribution with a slight notch burned into one side, as shown in the images on the top right. The double p echo train in red was acquired without hole burning and a plot of these echo maxima is shown on the lower right. Upon hole burning, the decay rate clearly increases, reflecting the ~1.5%

Hole Burning

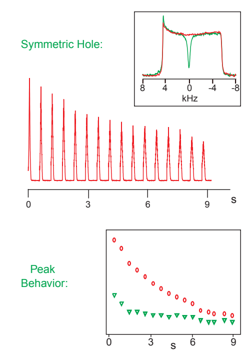

Trigger Detector

Burst Modulation

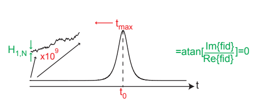

$<H_{1,N}^2> = 4kTR(Q/whA)^2$, giving: $H_{1,N}$ 260 pG

Nucleus	Conc.	N/cc	$H_{1,other}$
^1H	110 M	6.6×10^{22}	474 mG
^1H	1 mM	6×10^{17}	4.3 nG
^1H	50 M	3×10^{16}	216 pG
^{13}C	100 mM	6×10^{17}	268 pG

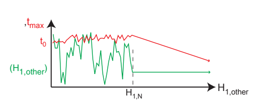

DRX 500 Nonideality

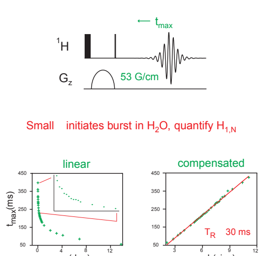

Small initiates burst in H_2O, quantify $H_{1,N}$

Estimate $H_{1,N}$ using $M_0 = 3.7\times10^{-2}$ A/m for H_2O

$H_{1,N} = \;_0M_0\sin\;_{min}$ 975 pG

Threshold Considerations

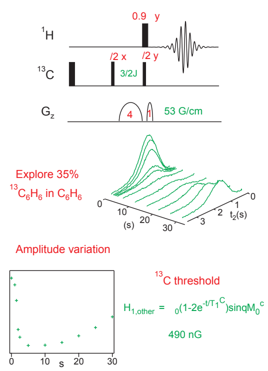

Explore 35% $^{13}C_6H_6$ in C_6H_6

Amplitude variation

^{13}C threshold

$H_{1,other} = \;_0(1-2e^{-t/T_1^C})\sin qM_0^C$

490 nG

Startup Considerations

Discussion of the time necessary for inverted magnetization $M(t=0) = -M_z$ to swing through the u-v plane and settle along the $+M_z$ direction begins with the Bloch equations for a single isochromat under conditions of radiation damping.

$$\frac{d}{dt}M_z = \;_2v + \;_1u + \frac{1}{T_RM_0}(u^2+v^2)$$

$$\frac{d}{dt}v = \;u + \;_2M_z \;\frac{1}{T_RM_0}M_zv \qquad \frac{d}{dt}u = \;v \;\;_1M_z \;\frac{1}{T_RM_0}M_zu$$

Here M_0 is the total magnetization, and the potentially time dependent Dw, w_1, and w_2 are the frequency offset, and the real, and imaginary components of an rf field. Notice that when $M(t=0) = -M_z$ and for $w_1 = w_2 = 0$, these equations predict that M(t) will remain along the $-M_z$ direction indefinitely. However, thermal noise in the rf circuit generates an incoherent rf field with components w_1 and w_2 near the Larmor frequency. It is this noise field that triggers formation of the usual super-radiant burst observed in concentrated samples following a perfect p pulse. To analyze this problem and calculate the time of the burst maximum t_{max} consider first the time behavior of the stereographic projection of M(t), G = v+iu/(1+Mz). Using the Bloch equations above one finds that G evolves according to the Ricatti equation.

$$\frac{d}{dt} = \frac{i}{2}(\;_1\;i\;_2)\;^2 + i\;\;\frac{1}{T_R}\;\;\frac{i}{2}(\;_1+i\;_2)$$

This equation is the key to an exact linearization of the Bloch equations under conditions of radiation damping. Now consider the evolutions of a two level spinor with amplitudes y_1 and y_2 under a complex rf field and corrected for radiation damping by forcing y_1 to grow and y_2 to decay at the rate $1/2T_R$.

$$\frac{d}{dt}\begin{pmatrix} 1 \\ 2 \end{pmatrix} = \frac{i}{2}\begin{pmatrix} +\frac{i}{T_R} & 1\;i\;2 \\ 1+i\;2 & \frac{i}{T_R} \end{pmatrix}\begin{pmatrix} 1 \\ 2 \end{pmatrix}.$$

Interestingly enough by defining $g = y_2/y_1$ and calculating the time behavior using the above matrix differential equation one recovers the Ricatti equation.

$$\frac{d}{dt} = \frac{i}{2}(\;_1\;i\;_2)\;^2 + i\;\;\frac{1}{T_R}\;\;\frac{i}{2}(\;_1+i\;_2)$$

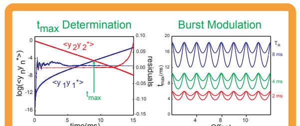

The similarity in the time behavior of g and G imply that the linear transformation of $y_1(0)$ and $y_2(0)$ into $y_1(t)$ and $y_2(t)$ via the 2x2 matrix on the left is equivalent to solving the nonlinear Bloch equations. Indeed one can predict u, v, and M_z at any time in terms of y_1 and y_2 via the ratio $G = g = y_2/y_1$ as $u + iv = 2G/(1+GG^*)$ and $M_z = (1-GG^*)/(1+GG^*)$. At t = 0 after a p rf pulse $M(t=0) = -M_z$, G = ¥, and one can take $y_2 = 1$ and $y_1 = 0$. In terms of a stochastic white noise excitation for w_1 and w_2 that is "discretized" by choosing a value at each time interval from a normal distribution with variance s^2/Dt the ensemble average $<y_1> = 0$ at all times for these initial conditions. This is consistent with experiment as both the burst time and phase are random producing zero average signal. Consider instead the evolution of the "density" $y_ny_m^*$ (where n,m = 1 or 2) by a matrix L derived from the 2x2 matrix on the left and its Hermitian conjugate. Note the similarity between the matrix elements of L and those one would expect on the basis of assigning y_1 and y_2 as |+> and |-> spin states. The presence of radiation damping is represented by gain and decay

$$L = \begin{pmatrix} \frac{1}{T_R} & \frac{i}{2}(\;_1+i\;_2) & \frac{i}{2}(\;_1\;i\;_2) & 0 \\ \frac{i}{2}(\;_1\;i\;_2) & i & 0 & \frac{i}{2}(\;_1\;i\;_2) \\ \frac{i}{2}(\;_1+i\;_2) & 0 & i & \frac{i}{2}(\;_1+i\;_2) \\ 0 & \frac{i}{2}(\;_1+i\;_2) & \frac{i}{2}(\;_1\;i\;_2) & \frac{1}{T_R} \end{pmatrix}$$

Again thermal noise in the circuit causes incoherent fluctuations in the rf field experienced by the magnetization. Modelling these changes in w_1 and w_2 with the same "discretized" white noise mentioned above now provides non-zero values for $<y_1y_1^*>$ and $<y_2y_2^*>$. In terms of the time step weighted variance $(s^2/Dt)Dt$, the time evolution of these components is given by:

$$\frac{d}{dt}\begin{pmatrix} \langle 1\;1^* \rangle \\ \langle 2\;2^* \rangle \end{pmatrix} = \begin{pmatrix} \frac{1}{T_R}\;\frac{2}{2} & \frac{2}{2} \\ \frac{2}{2} & \frac{1}{T_R}\;\frac{2}{2} \end{pmatrix} \times \begin{pmatrix} \langle 1\;1^* \rangle \\ \langle 2\;2^* \rangle \end{pmatrix}$$

The numerical average of $<y_1y_1^*>$ and $<y_2y_2^*>$ over 1000 particles is shown graphically as thick lines in the top left graph for T_R = 2 ms, s^2 = 0.5 rad^2/ms^2, and Dw = 0.5 rad/ms. An analytical solution based on the above matrix equation yields curves essentially identical to those shown on the figure. The residuals between numerical computation of $<y_1y_1^*>$ and $<y_2y_2^*>$ and the approximation are also included in this diagram to demonstrate the accuracy of this analytical model. Comparison of the intersection point of these two curves with single particle values for y_1 indicates that this particular time describes the average burst time t_{max}. Equating the analytical solutions deduced from the above matrix equation yields the startup time as

$$t_{max} = \frac{1}{\sqrt{\frac{4}{4}+\frac{1}{T_R^2}}}\tanh^{-1}\left(\frac{\sqrt{\frac{4}{4}+\frac{1}{T_R^2}}}{\frac{2}{2}+\frac{1}{T_R}}\right) \quad T_R\ln\left(\frac{2}{\sqrt{T_R}}\right)$$

It is interesting to ask how much coherent rf field is necessary to dominate and shorten t_{max} to determine whether or not a trigger based detection strategy is possible. Proceeding in exactly the same way as above in the determination of $<y_1y_1^*>$ and $<y_2y_2^*>$ leads to the relation

$$t_{max} \quad T_R\ln\left(\frac{2}{\sqrt{\;^2T_R + \frac{\;_1^2+\;_2^2}{\;^2+\frac{1}{T_R^2}}}}\right)$$